Available online at www.sciencedirect.com

SCIENCE DIRECT

Materials Letters 59 (2005) 4034 – 4037

materials letters

www.elsevier.com/locate/matlet

Hydrothermal synthesis of alumina nanotubes templated by anionic surfactant

Lihong Qu, Changqing He, Yue Yang, Yanli He, Zhongmin Liu *

Dalian Institute of Chemical Physics, Chinese Academy of Sciences, Dalian 116023, P.R. China

Received 15 December 2004; accepted 22 July 2005
Available online 3 August 2005

Abstract

The alumina nanotubes were prepared by using the anionic surfactant, sodium dodecyl sulfonate (SDS), as structure-directing template for the first time with $Al(NO_3)_3{\cdot}9H_2O$ as precursor via a hydrothermal method. Structure and morphology of the nanotubes were characterized by XRD, TEM, FT-IR, TG and N_2 adsorption–desorption. The obtained nanotubes were found having outer diameters from 6 to 8 nm with length up to 200 nm.

Keywords: Anionic surfactant; Alumina; Nanotubes; Hydrothermal synthesis; Characterization

1. Introduction

Since the discovery of carbon nanotubes by Iijima [1], much attention has been paid to the preparation, property and application of these materials. Based on uniquely electronic, mechanical and chemical properties of carbon nanotubes with marked shape-specific and quantum size effects [1–3], nanotubular materials are expected to exhibit both unusual characteristics and potential applications [4]. During the last decade, various nanotubes have been prepared, inclusive of Bi [5], TiO_2 [6], SiO_2 [7], Al_2O_3 [8], MX_2 (M∼Mo, W, Nb, Ta; X∼S, Se) [9,10], VO_x [11,12], $NiCl_2$ [13], $H_2Ti_3O_7$ [14], AlN [15], rare earth (Er, Tm, Yb, Lu) oxides [16] and so on. Most recently, considerable efforts have been directed towards the preparation of nano-structured alumina, due to their novel properties, such as high elastic modulus, thermal and chemical stability, and optical characteristics [14]. Up to date, nanosized Al_2O_3 with different morphologies, such as nanotubes [8,17–21], nanowires [22], nanobelts [22], nanofibers [23,24], rod-shaped nanoparticles [25] and whiskers [26], has been synthesized by a variety of routes. However, there has been no report on the formation of nanotubular alumina in the presence of the anionic surfactant, sodium dodecyl sulfonate (SDS), as structure-directing agent. In this work, we first report successful synthesis of alumina nanotubes templated by sodium dodecyl sulfonate.

2. Experimental

The synthesis of alumina nanotubes was carried out via a simple hydrothermal method. A typical procedure is described as follows: 2.8 g of sodium dodecyl sulfonate was dissolved into 70 g of distilled water at 50 °C to prepare solution A. 22.9 g of $Al(NO_3)_3{\cdot}9H_2O$ was dissolved in 40 g of distilled water at room temperature to achieve solution B. Solution B was slowly added into solution A under stirring, and the mixture was continuously stirred for several minutes at 50 °C. Thereafter, 12.0 g of aqueous ammonia was dripped into the mixture until pH value of 5.0–5.5. After being stirred for additional several minutes, the resulting suspension was transferred into a Teflon-lined autoclave (100 ml), and heated at 120 °C for 90 h. After the completion of hydrothermal treatment, the autoclave was cooled down to room temperature naturally, and the solid product was recovered by centrifuge, washed several times with a

* Corresponding author. Tel.: +86 411 84685510; fax: +86 411 84379289.
E-mail address: liuzm@dicp.ac.cn (Z. Liu).

0167-577X/$ - see front matter © 2005 Elsevier B.V. All rights reserved.
doi:10.1016/j.matlet.2005.07.059

solution consisting of distilled water and 95% ethanol, and finally dried at 50 °C overnight. The template in the solids was removed by calcinations and extraction, respectively. During calcinations, the sample was heated in air from room temperature to a certain temperature in the range of 500–800 °C with a temperature ramp of 1 °C min^{-1}, and kept at that temperature for 5 h. 0.2 M ethanol solution of ammonium acetate was used to perform the solvent extraction at room temperature for 4 days while stirring.

The structure of samples was determined by powder X-ray diffraction (XRD) on a Rigaku D/max-b X-ray powder diffractometer with Cu $K\alpha$ radiation ($\lambda = 1.5418$ Å) in the scan range of 1–50° 2θ. The morphology of samples was characterized by transmission electron microscopy (TEM) using a JEOL-JEM-2000EX apparatus with an accelerating voltage of 100.0 kV. Prior to TEM measurements, the samples were ultrasonically dispersed into anhydrous ethanol for 5 min. IR vibration spectra (KBr pellet) were recorded at ambient temperature on a Bruker EQUINOX 55 FT-IR spectrometer with a resolution of 4 cm^{-1}. Thermogravimetry (TG) analysis measurement was recorded on a Perkin Elmer Pyriss TGA equipment with a temperature rate of 10 °C min^{-1} from 50 to 900 °C under air gas with a flow rate of 20 ml min^{-1}. Nitrogen adsorption–desorption isotherms were measured on a Micrometritics ASAP-2010 apparatus at 77 K. Prior to adsorption analysis, samples were degassed for at least 6 h at given temperatures. BET surface area was calculated based on the adsorption data in the relative pressure range of $p/p_o = 0.05–0.25$, pore volume was estimated from volume adsorbed at a relative pressure of 0.99. Mesopore size distribution was calculated from desorption branch by BJH method, while micropore diameter was estimated by HK method.

3. Results and discussion

TEM images of as-synthesized and treated samples are shown in Fig. 1. Very obviously, individuals and aggregates of nanotubes

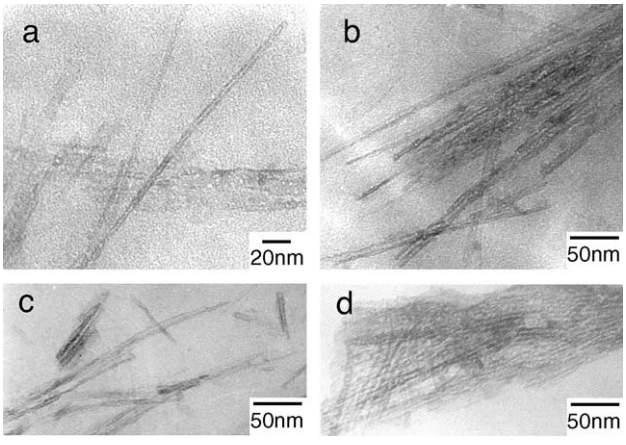

Fig. 1. TEM images of samples: (a) and (b) as-prepared, (c) solvent-extracted, and (d) calcinated at 500 °C for 5 h.

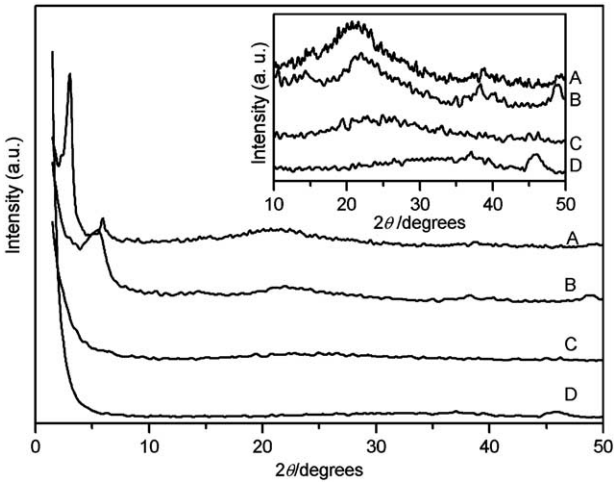

Fig. 2. XRD patterns of samples: (A) as-prepared, (B) solvent-extracted, (C) calcined at 500 °C and (D) at 800 °C.

can be observed. For as-synthesized samples, outer diameter of most of nanotubes is 6–8 nm and length is up to 200 nm (Fig. 1a and b). After being extracted by solvent at room temperature, the diameter of nano-tubes was about 3–10 nm (Fig. 1c). However, the calcination treatment at 500 °C resulted in the ruin of nanotubes without the presence of any visible isolated or agglomerated nanotube, but slit-like pores (Fig. 1d).

The crystalline phase of nanotubes was identified by powder X-ray diffraction. Fig. 2 shows XRD patterns of samples, in which inserted diagrams represent the enlarged curves in the range 10°–50° 2θ. Two clear and intense diffraction peaks at around 3° and 6° can be observed from XRD pattern of as-prepared product with a broad band at around 20° assigned to amorphous alumina (curve A of Fig. 2). This indicates that uniformly mesostructured alumina has been obtained under our experimental conditions, in agreement with the observation from TEM image. It is rather profound that the diffraction peaks at the low angle ($2\theta < 6°$) have not been observed for alumina nanotubes to date [8,17–21], but a similar phenomenon was reported in the case of erbium oxide nanotubes [16]. As displayed in curve B of Fig. 2, a diffraction peak emerges at *ca.* 5° 2θ for the solvent-extracted sample, together with an observable framework feature of amorphous alumina and boehmite. Compared with the as-prepared sample, the first peak at *ca*. 3° disappears, the second peak shifts toward high *d*-spacing and broadens, showing that solvent extraction retards the long-range ordering of the as-prepared sample, as proven by uneven nanotubular image (Fig. 1c). After being calcined, the diffraction at low angle cannot be observed at all, suggesting the complete loss of long-range ordering. The calcinations at 500 °C led to amorphous solid, and the treatment at 800 °C to γ-Al_2O_3, in agreement with the phase transformation of alumina upon thermal treatment that alumina hydrate dehydrated to amorphous alumina at the temperature between 200 and 700 °C, and further to γ-Al_2O_3 at 800 °C [27].

The FT-IR vibration spectrum of as-prepared nanotubes (curve A of Fig. 3) has two strong adsorptions at 2926 and 2856 cm^{-1} assigned to $-CH_2-$ group, one at 2957 cm^{-1} to $-CH_3$ group, and both at 1167 and 1051 cm^{-1} to $-SO_3^-$ group, indicating the incorporation of SDS into nanotubular solid. However, the aforesaid absorbance bands totally disappear in the IR spectrum of solvent-extracted solid (curve B of Fig. 3), suggesting the complete removal of the template.

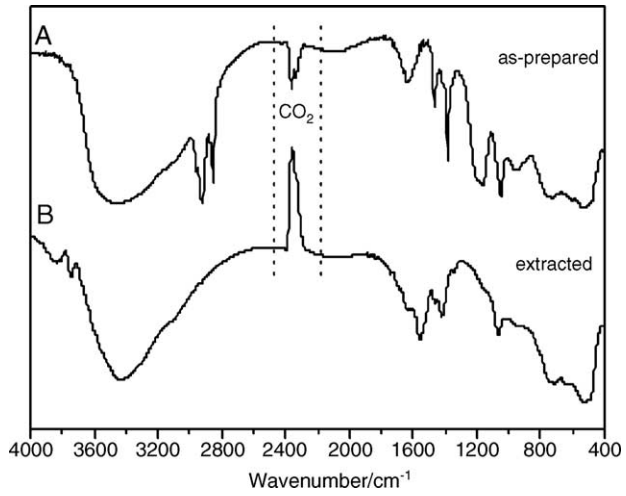

Fig. 3. IR spectra of samples: (A) as-prepared, (B) solvent-extracted.

The thermal stability of the alumina nanotubes was studied by thermal gravity analysis in air atmosphere. Fig. 4 shows the TG/DTG curves of some representative as-made nanotubes. It is found that six distinct steps of weight loss are discernible, in the range of (I) $t<110$ °C, (II) 110 °C$<t<$201 °C, (III) 201 °C$<t<$397 °C, (IV) 397 °C$<t<$600 °C, (V) 600 °C$<t<$800 °C and (VI) $t>800$ °C. The first step with a weight loss of 7.20% can be attributed to the desorption of dissociated water, and then the second step with 5.75% loss corresponds to the removal of water loosely bounded. While the temperature increasing, the removal of the template takes place. Sicard reported that the alkyl chain of surfactant, sodium dodecylsulfate, was completely removed below 200 °C, whereas the sulfate head group was lost in the region between 400 and 600 °C [28]. Similar phenomenon was found in our experiment. The major loss of 31.17% in step

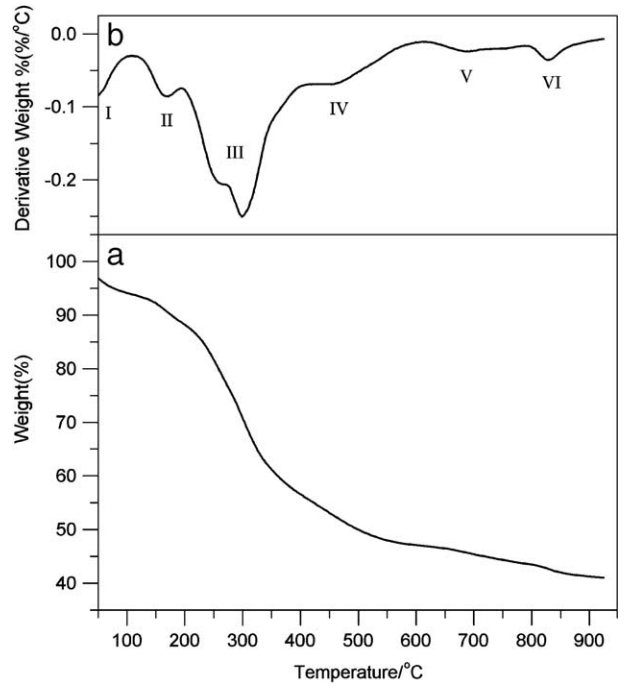

Fig. 4. TGA/DTG curves of alumina nanotubes.

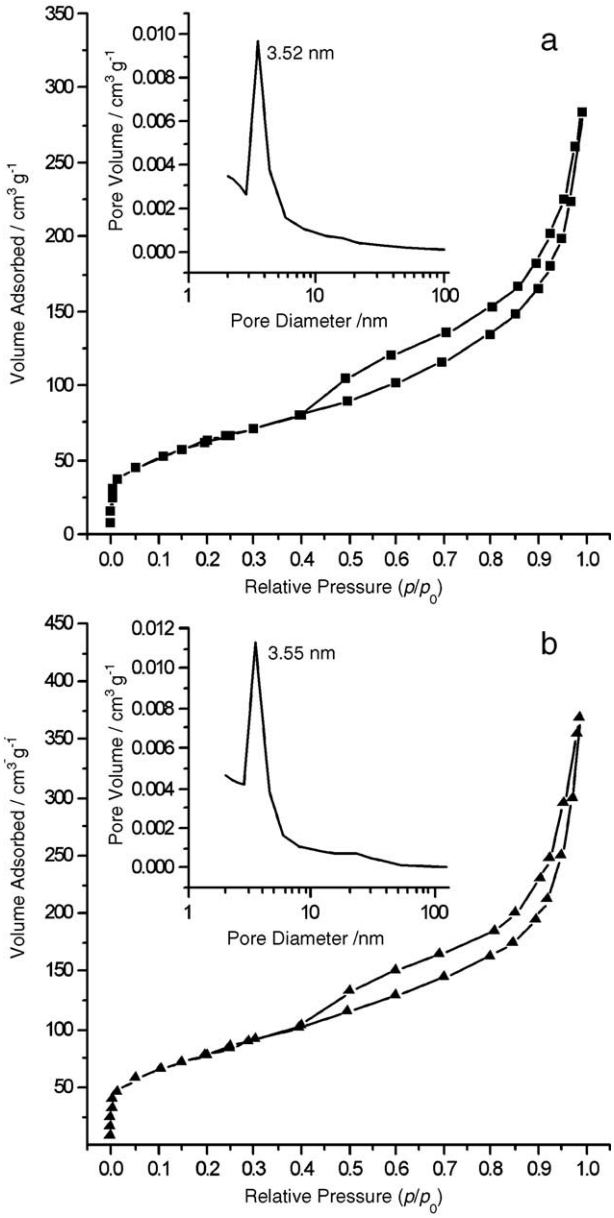

Fig. 5. N_2 adsorption–desorption isotherms and pore size distributions of samples: (a) extracted, (b) calcinated at 500 °C for 5 h.

III can be attributed to the removal of the alkyl chain of SDS, and the weight loss of 9.79% in step IV to the loss of the sulfonate head group. The different removal temperature of alkyl chain may be caused by the difference of head groups. While calculated from the data of weightlessness in steps III and IV, the weight loss ratio of the former to the later is 3.19, which is far from the stoichiometric ratio of alkyl chain to sulfonate head group in

Table 1
BET data of samples

Sample	S_{BET} (m^2 g^{-1})	Pore Volume (cm^3 g^{-1})	D_{meso} (Å)	D_{micro} (Å)
Solvent-extracted	225.4	0.44	35.2	7.2
Calcined	287.0	0.57	35.5	6.5

SDS. Therefore, the major loss of 31.17% may be caused not only by the removal of the alkyl chain of the surfactant but also by the loss of water in the amorphous alumina framework. While the temperature exceeds 600 °C, the amorphous alumina dehydrate to a transitional phase and further to γ-Al_2O_3, coinciding with the XRD results (Fig. 2).

Fig. 5 shows N_2 adsorption–desorption isotherms for samples extracted by solvent and calcined at 500 °C, which look rather similar. At the low relative pressure (p/p_o=0–0.40), *type I* adsorption behavior is observed, with a rapid increase of adsorption amount, typical of the characteristics of microporous materials [29]. However, a *type IV* isotherm with a type H_3 hysteresis loop appears at the relative pressure range of 0.4–0.99, characteristic of mesoporous solids, where type H_3 hysteresis loop at high relative pressure (p/p_o) is often associated with the formation of aggregates with slit-shaped pores, i.e. a loosely coherent assembly of particles. Generally, the adsorption on isotherm at the low pressure can be assigned to the monolayer coverage of mesopores and particle surface, the adsorption at the medium pressure (p/p_o=0.40–0.85) mainly due to capillary condensation of N_2 in mesopores, while that at the high pressure (p/p_o=0.85–0.99) is likely contributed by aggregated pores. BET data of both solids are summarized in Table 1.

The existence of micropores suggests the formation of cavities inside the multi-wall of nanotubes, possibly resulting from the removal of water, template and gas molecules adsorbed. For the calcined sample, a narrow mesopore size distribution (2–5 nm) measured by N_2 adsorption–desorption isotherm was close to the value observed by TEM, but in the case of the solvent-extracted one, no any appreciable mesopore size distribution was obtained by the same route. It was noticed that the solvent-extracted sample that had undergone the process of degassing and N_2 adsorption–desorption at 77 K did not represent any visible XRD peak at *ca*. 5° 2θ (not shown here), possibly imposed by the negative effect during degassing and measurement.

4. Conclusions

Alumina nanotubes have been synthesized successfully by using sodium dodecyl sulfonate as structure-directing agent via a hydrothermal method. Further elucidation on the stability of nanotubes is in progress. Alumina nanotubes are expected to find potential applications in catalysis, adsorption/separation and nano-device.

References

[1] S. Iijima, Nature 354 (1991) 56.
[2] Issues in nanotechnology, Science 290 (2000) 1523.
[3] P.M. Ajayan, T.W. Ebbessen, Rep. Prog. Phys. 60 (1997) 1025.
[4] R.H. Baughman, A.A. Zakhidov, W.A. de Heer, Science 297 (2002) 787.
[5] Y. Li, J. Wang, Z. Deng, Y. Wu, X. Sun, D. Yu, P. Yang, J. Am. Chem. Soc. 123 (2001) 9904.
[6] H. Imai, Y. Takei, K. Shimizu, M. Matsuda, H. Hirahima, J. Mater. Chem. 9 (1999) 2971.
[7] M. Harada, M. Adachi, Adv. Mater. 12 (2000) 839.
[8] B.C. Satishkumar, A. Govindaraji, E.M. Vogl, L. Basumallick, C.N.R. Rao, J. Mater. Res. 12 (1997) 604.
[9] Y. Li, X. Li, R. He, J. Zhu, Z. Deng, J. Am. Chem. Soc. 124 (2002) 1411.
[10] M. Nath, C.N.R. Rao, J. Am. Chem. Soc. 123 (2001) 4841.
[11] F. Krumeich, H.-J. Muhr, M. Niederberger, F. Bieri, B. Schnyder, R. Nesper, J. Am. Chem. Soc. 121 (1999) 8324.
[12] X. Chen, X. Sun, Y. Li, Inorg. Chem. 41 (2002) 4524.
[13] Y. Rosenfeld Hacohen, E. Grunbaum, R. Tenne, J. Sloan, J.L. Hutchison, Nature 395 (1998) 336.
[14] Q. Chen, W. Zhou, G. Du, L. Peng, Adv. Mater. 14 (2002) 1208.
[15] Q. Wu, Z. Hu, X.Z. Wang, Y.N. Lu, X. Chen, H. Xu, Y. Chen, J. Am. Chem. Soc. 125 (2003) 10176.
[16] M. Yada, M. Mihara, S. Mouri, M. Kuroki, T. Kijima, Adv. Mater. 14 (2002) 309.
[17] L. Pu, X. Bao, J. Zou, D. Feng, Angew. Chem., Int. Ed. Engl. 40 (2001) 1490.
[18] J. Zou, L. Pu, X. Bao, D. Feng, Appl. Phys. Lett. 80 (2002) 1079.
[19] D. Kuang, Y. Fang, H. Liu, C. Frommenb, D. Fenske, J. Mater. Chem. 13 (2003) 660.
[20] H.C. Lee, H.J. Kim, S.H. Chung, K.H. Lee, H.C. Lee, J.S. Lee, J. Am. Chem. Soc. 125 (2003) 2882.
[21] H.J. Kim, H.C. Lee, C.H. Rhee, S.H. Chung, H.C. Lee, K.H. Lee, J.S. Lee, J. Am. Chem. Soc. 125 (2003) 13354.
[22] X.S. Peng, L.D. Zhang, G.W. Meng, X.F. Wang, Y.W. Wang, C.Z. Wang, G.S. Wu, J. Phys. Chem., B 106 (2002) 11163.
[23] V. Valcárcel, A. Pérez, M. Cyrklaff, F. Guitián, Adv. Mater. 10 (1998) 1370.
[24] H.Y. Zhu, J.D. Riches, J.C. Barry, Chem. Mater. 14 (2002) 2086.
[25] Z. Zhang, R.W. Hicks, T.R. Pauly, T.J. Pinnavaia, J. Am. Chem. Soc. 124 (2002) 1592.
[26] Z. Yu, Y. Du, J. Mater. Res. 13 (1998) 3017.
[27] X. Zhao, Catalyst, China Logisties Publishing House, Beijing, 2001, p. 573.
[28] L. Sicard, P.L. Llewellyn, J. Patarin, F. Kolenda, Micro. Meso. Mater. 44-45 (2001) 195–201.
[29] K.S.W. Sing, D.H. Everett, R.A.W. Haul, L. Moscou, R.A. Pietotti, J. Rouquerol, T. Siemienieska, Pure Appl. Chem. 57 (1985) 603.